2004

Geometrical Optimisation of a Rotary Compressor for Refrigerators

Kim Tiow Ooi
Nanyang Technology University

GEOMETRICAL OPTIMISATION OF A ROTARY COMPRESSOR FOR REFRIGERATORS

KT Ooi
Ph.D, Associate Professor
Thermal and Fluids Engineering Division
School of Mechanical and Production Engineering
Nanyang Technological University
50 Nanyang Avenue, Singapore 639798

Tel: (65) 6790-5511, Fax: (65) 6792-4062, Email:mktooi@ntu.edu.sg

ABSTRACT

The rolling piston has been widely used in refrigeration and air-conditioning industries. It is a geometrically simple machine with only four basic parts: a cylinder, roller, a vane and a vane spring. Its performance depends on the balance amongst heat transfer, fluid flow and mechanical aspects of the machine. In this study, effort has been focused on improving the coefficient of performance of the compressor (COP) by improving its mechanical performance. A lumped mathematical model for the compressor has been formulated to predict the overall performance of the machine. The model accounts for geometrical dimensions, operating conditions, valve dynamics, thermodynamics aspects, flow and mechanical losses. The prediction of the model has been compared with measured results and good agreement has been obtained. The model has been linked with an optimisation algorithm to search for a combination of some 12 design variables together with 20 sets of design constraints for an optimum compressor performance in terms of reduced mechanical losses and hence improved the COP of the machine. A constrained multi-variable direct search optimisation technique has been employed. Theoretical studies suggest that a total reduction of mechanical losses of 70% is possible and this brings about an overall improvement in the COP of the compressor of 14%.

1. INTRODUCTION

The rolling piston compressor has been widely used in the refrigeration and air conditioning industries since early 1980s. It attracted a lot of attention from the industries and research centres in 1980-1990s. More recent comprehensive theoretical and experimental studies are available in the literature [1-11].

Fig. 1 shows a pump and electrical motor assembly for a typical rolling piston compressor used in refrigerators. In its basic form, the pump assembly consists of 4 main parts: a stator, a roller piston, a vane and a vane-spring. During operation, the roller rotates and two working chambers formed by the stator inner wall, the roller and the vane. During the operation, these chambers change in size and hence results in compression and expansion of the working fluid which forms a complete compressor working cycle. A typical cycle takes two motor revolutions to complete. The design of the compressors is constantly reviewed into for further performance improvement. With the advancement in computer technology, computerized design optimization procedures have been used to speed up the design process and improve performance. The paper presents an 12-variable design optimisation aims to increase the COP of a refrigeration rolling piston compressor, under preset operational conditions and some 20 sets of design constraints.

2. MATHEMATICAL MODEL

In the following sections, a brief account of the mathematical model will be presented. A more comprehensive treatment of the can be found in refs. [1,8].

2.1 GEOMETRICAL MODEL

The volume of the working chamber [9], taking into consideration of the vane thickness, can be shown as:

$$V(q) = \frac{l\,R_c^2}{2}\left[(1-a^2)q - \frac{(1-a)^2}{2}\sin 2q - a^2 \sin^{-1}\left\{\left(\frac{1}{a}-1\right)\sin q\right\} - a(1-a)\sin q\sqrt{1-\left(\frac{1}{a}-1\right)^2 \sin^2 q}\right]$$

$$-\frac{t_b\, h_b}{2} R_c \left\{ 1 - (1-a)\cos q - \sqrt{(1-a)^2 \cos^2 q + 2a - 1} \right\} \tag{1}$$

2.2 Thermodynamic processes

The inter-relationships among temperature, pressure and mass are given by equations (2), (3) and (4).

$$\frac{dT_c}{dt} = \frac{\frac{1}{m_c}\left[\frac{dQ}{dt} + \sum \frac{dm_i}{dt}(h_i - h_c) - \sum \frac{dm_o}{dt}(h_o - h_c)\right] + \frac{dv_s}{dt}\left[v_c \left(\frac{\P p_c}{\P v_s}\right)_T - \left(\frac{\P h_c}{\P v_c}\right)_T\right]}{\left[\left(\frac{\P h_c}{\P T_c}\right)_{v_s} - v_c \left(\frac{\P p_c}{\P T_c}\right)_{v_s}\right]} \tag{2}$$

$$\frac{dp_c}{dt} = \left(\frac{\P p_c}{\P T_c}\right)_{v_s} \frac{dT_c}{dt} + \left(\frac{\P p_c}{\P v_c}\right)_T \frac{dv_s}{dt} \tag{3}$$

$$\sum \frac{dm_i}{dt} - \sum \frac{dm_o}{dt} = \frac{dm_c}{dt} \tag{4}$$

The significance of heat transfer, Q on compressor performance, has been debated by several researchers [9-11]. In this project however, heat transfer effect is excluded to reduce computational time. The accuracy of the prediction has been verified with measured results and good accuracy is obtained, as shown Table 1.

2.3 Mass flow through valve

The compressor simulation assumes that the flow through valves is a steady one-dimensional adiabatic flow. Thus, the mass flow through valves can be expressed as

$$\frac{dm_2}{dt} = \frac{C_d A_2 \sqrt{2(h_1 - h_{2s})}}{v_{s2}} \tag{5}$$

where C_d indicates the combined effect of non-isentropic and flow losses [8].

The area of the valve requires that the valve opening to be known at any point of time. This is obtained by solving the valve dynamic behaviour, the details of which is available ref [7].

To solve eqns. (1) to (5), it is necessary for the gas properties and their respective derivatives to be determined. In this study, R22 is used as the working fluid and its properties are taken from reference [12], from which the pressure, enthalpy and other derivatives [8] for the gas properties can be obtained.

2.4 Frictional losses

One of the important factors affecting the performance of the compressor is the friction between the rubbing parts. In the simulation model [8], there are seven areas of concern and these are:

i. Frictional loss between the eccentric and the inner surface of the roller, L_{er}:

$$L_{er} = (w - w_r)\frac{2ph(w - w_r)lR_e^{\,3}}{d_2} \tag{6}$$

ii. Frictional loss between the roller face and the cylinder head faces, L_{rc}:

$$L_{rc} = w\frac{2pw_r h\left(R_r^{\,4} - R_e^{\,4}\right)}{d_1}{}_r \tag{7}$$

iii. Frictional loss between eccentric face and the cylinder head faces, L_{ec}:

$$L_{ec} = w\frac{pw^2 h\left((R_s + d_f)^4 - R_s^{\,4}\right)}{d_3} \tag{8}$$

iv. Frictional loss between vane tip and roller, L_v:

$$L_v = F_{vt} R_r w_r + \frac{ew\cos q}{\cos a} \tag{9}$$

v. Frictional loss between vane sides and vane slot, see Fig. 2(b), L_s:

$$L_s = (F_{t1} + F_{t2})\dot{x} \tag{10}$$

vi. Frictional loss between shaft and bearing S, L_{bs}:

$$L_{bs} = w\frac{2phw\, l_{bs} R_s^{\,3}}{d_4} \tag{11}$$

vii. Frictional loss between shaft and bearing L, L_{bl}:

$$L_{bl} = w \frac{2phw\, l_{bl} R_s^{\,3}}{d_5} \tag{12}$$

The total frictional loss is obtained by summing up all the losses shown in equations (6) to (12).

The above equations show that, among other parameters, the frictional analysis is dependent significantly on the eccentric radius R_e, the roller radius R_r , the cylinder radius R_c and the shaft radius, R_s and the height of the cylinder, l (note that the height of the cylinder is also same as the height of the vane, h_b). All these parameters should be included in the optimization study as free variables. Free variables are variables that are allowed to vary during an optimization search.

3. COMPRESSOR OPTIMISATION

In this study, the objective function involved in the current optimisation study is highly non-linear and may not be differentiable. Therefore a direct search method introduced by M.J. Box [13] was employed. This method is a sequential technique that has proven effective in solving problems with non-linear objective functions. In general, an optimisation study can be mathematically represented by:

$$\text{Maximise: } F(x) = f(x_1, x_2, ..., x_N) \tag{13}$$

Subject to:

$$\text{(i) } L_E(x)_i \leq E(x)_i \leq H_E(x)_i, i = 1,2,.....N \tag{14}$$

$$\text{(ii) } L_G(x)_j \leq G(x)_j \leq H_G(x)_j \;\; j = 1,2,......, M \tag{15}$$

where E and G are the explicit constraints and geometrical constraints, respectively, L and H represent the lower and higher limit, I and j are the number of explicit and geometrical constraints, respectively.

The details Box COMPLEX method will not be shown here, it can be referred to ref [13].

3.1 Objective function and constraints

The objective function for this optimisation study is coefficient of performance (COP), which is effectively the overall performance figure for the compressor. This is carried out at the given operational conditions and at a fixed capacity of the compressor.

Mathematically, this is defined as:

$$\text{Maximise } f_{\text{obj}} = f(R_{SB}, R_{IB}, R_c, R_r, R_e, D_{sp}, D_{dp}, K_s, V_t, V_w, V_l, V_r) \tag{16}$$

Subject to the following constraints:

$$x_l(i) < x(i) < x_h(i) \;,\; i = 1,2...,12 \tag{17}$$

where x(i) are the free variables, x_l(i) and x_h(i) are lower and upper limits of the free variables, respectively. The free variables used are shown in Table 3.

In this case the value of COP will be maximised during the optimisation search. In eqn. (17), $x(i)$, $i = 1,2..,12$ are design variables R_{SB}, R_{LB}, R_c, R_r, R_e, D_{sp}, D_{dp}, K_s, V_t, V_w, V_l, V_r, respectively. The values of $x_l(i)$ and $x_h(i)$ are lower and upper limits of the design variables, call explicit constraints. This defines the region in which feasible designs are located. Table 3 tabulates the values of the constraints. The geometrical constraints are also specified to ensure that the final geometries are feasible and these are:

$$g_l(j) < gx(j) < g_h(j) \;,\; j = 1,2...8 \tag{18}$$

where $g(i)$, $i = 1..8$ are the geometrical constraint. The $g_l(j)$ and $g_h(j)$ are the lower and upper limits of the geometrical constraints. In this study, the constraint is specified to ensure that the volumetric displacement of the compressor is constant, such that the capacity of the compressor remains constant throughout the optimisation search. The constant swept volume is achieved by varying the cylinder height in accordance with the following relationship:

$$h_b = \frac{V_{swept}}{\left(\frac{p\left(D_c^{\ 2} - D_r^{\ 2}\right)}{4}\right)} \qquad (19)$$

where V_{swept} is the preset swept volume the compressor should have in order to fulfil the capacity requirement. The cylinder height h_b is varied according to eqn (19) during the optimisation search.

The constraints is also set such that the eccentric diameter must be conformed to eqn (20).

$$D_e > (D_c - D_r + D_s) \qquad (20)$$

where D_s is the min of the D_{SB} or $D_{IB.}$
Table 4 shows the geometric constraints applied. These constraints ensure that geometrical configuration of the compressor is feasible in practical situations.

4. RESULTS AND DISCUSSIONS

In this study, the operational conditions of the compressor are:

Speed (RPM)	:3000.000 RPM		
Inlet Temp.(Ts)	: 340.850 K	Discharge Temp.(Td)	: 400.150 K
Suction Press. (Ps):	215.671 kPa	Discharge Press.(Pd):	2146.992 kPa

The optimization search was implemented on an IBM PC equipped with 2.6 GHz Pentium processor and the optimization search took 1 hours to complete.

Figs. 2 to 5 show the results for the optimization study. The results are normalised with respect to the parameters of the first initial complex. Fig. 2(a) shows that the objective function increases by about 14% at the end of the optimisation search. Figure 2(b) shows that the whole searching process makes a total of 338 model evaluation and out of which 211 are successful iterations. Successful iteration refers to model evaluation that yields improvement in the value of the objective function and the compressor design is fallen within all the imposed constraints. Figs. 2(c) and 2(d) shows that the S and L bearing diameters converged to the lower limits imposed. The reduction in these diameters results in 37% reduction in fictional loss at these two locations, as shown in Table 5.

Figs. 2(e) and 2(f) show that the roller and cylinder diameters reduced by more than 15% each and this has resulted in the cylinder height to increase by 30%, resulting in a much longer compressor, as shown in Fig. 2(g). Eccentric diameter is calculated from D_s-D_r + D_s and its variation is shown in Fig. 2(h). The increase in the eccentric diameter does not increase the friction between the eccentric and the cylinder end face as there is an undercut at the eccentric face. The friction in this location is in fact reduces, as shown in Table 5.

Figures 2(i) and (j) shows that both suction and discharge port diameters increase and cause reductions in suction and discharge losses. Figs. 2(k) to 2(n) show variations of valve dimensions. The results show that the optimum valve design is easier to open as it is thinner, narrower and longer, which has the effect of reducing valve loss. In practice, the final valve design must be checked using the fatigue analysis to prevent premature valve failure. Fig. 2(o) shows that the vane-spring gets stiffer, which has resulted in a significant increase in the valve tip loss. But as the absolute value is small, such an increase does not result in any noticeable change in compressor performance.

Table 5 summarises the overall change in compressor design variables as well as the resulted changes in compressor performance parameters.

5. CONCLUSION

The study demonstrated that a design optimization algorithm coupled with the mathematical model of the compressor is a useful tool in compressor design. It can effectively suggest a set of dimensions that produces optimum compressor performance based on the design requirement. The study suggests that, for this design, based on the criteria of maximising COP, a narrower but taller cylinder is a better design. The model suggests that more than 70% reduction in the mechanical loss is possible through a proper combination of design dimensions. This gives an overall improvement of COP of 14%, as the shaft power input reduces due to lower frictional losses and lower suction and discharge losses.

NOMENCLATURE

α	R_r/R_c
A	valve Flow Area, m^2
C_d	discharge coefficient
e	eccentricity, Rc-Rr, m
F_x	net pressure force on vane in x-direction, N
F_y	net pressure force on vane in y-direction, N
F_{vt}	tangential force at vane tip, N
F_{vn}	normal force at vane tip, N
F_{t1}, F_{t2}	tangential forces at vane side contact points, N
F_{n1}, F_{n2}	normal forces at vane side contacts, N
h	specific enthalpy, J/kg
h_b	vane height, m
h_{2s}	downstream isentropic enthalpy, kJ/kg
k_s	vane spring constant, N/m
l	cylinder length (also roller length,), m
l_{bl}	length of bearing L, m
l_{bs}	length of bearing S, m
m	mass of fluid, kg
$\dot{m}$	mass flow rate, kg/s
N	rotational speed of compressor, rev/min
P	pressure, bar or N/m^2
P_b, P_c	pressure in suction and compression chamber, bar or N/m^2
P_s, P_d	suction and discharge pressure, bar or N/m^2
Q	heat transfer rate, W
R_c	cylinder radius, m
R_r	outer roller radius, m
R_e	radius of eccentric, m
R_{SB}	S-Bearing radius, m
R_{LB}	S-Bearing radius, m
T	temperature, K
t_b	vane thickness, m
V	volume, m^3
v_s	specific volume, m^3/kg
W	work, J
$\dot{x}$	vane velocity, m/s

Greek letters

θ	angular position of rotor/crankshaft, rad
α	offset angle of rolling piston centre, rad
δ_1	clearance at roller and cylinder, m
δ_2	clearance at eccentric and roller, m
δ_3	clearance at eccentric and cylinder, m
δ_4	clearance at shaft and bearing S, m
δ_5	clearance at shaft and bearing L, m
δ_f	eccentric face land width, m
η	viscosity of lubricating oil, Ns/m^2
η_{se}	isentropic efficiency
ω	angular velocity of crankshaft, rad/s
ω_r	angular velocity of roller, rad/s
ρ	density, kg/m^3

Subscripts

i	inlet (suction) conditions
o	outlet (discharge) conditions
1	upstream conditions
2	downstream conditions
c	cylinder chamber properties/conditions
s	suction
d	discharge

REFERENCES

(1) G. Prater Jr, Computer modeling and simulation of stationary-vane, rolling piston refrigeration compressors. *Computer Modeling in Engineering & Sciences*, 3(3), 299-312 (2002)

(2) G. Prater Jr, et al. Optical measurement of discharge valve modal parameters for a rolling piston refrigeration compressor. *Journal of the International Measurement Confederation*, 33(1), 2003, 75-84 (2003)

(3) D. Manole, Refrigerant dependent optimum clearance for rotary compressors, *Sixteenth Int'l Compressor Engineering Conf.* At Purdue, C5-2 (2002)

(4) H. J. Kim and J. M. Ahn, Numerical study on the lubrication oil distribution in a refrigeration rotary compressor, *Int. J. Refrig.* 26(3), 800-808 (2003)

(5) J.Wu, Dynamic Analysis of roller and vane of inverter controlled rotary compressors, *Proc. International Compressor Engineering Conf.*, Purdue University, (1) 287-294 (2000)

(6) J.L. Gzasche, Two Phase flow of oil-refrigerant mixture through the radial clearance in rolling piston compresors, *Proc. International Compressor Engineering Conf.* At Purdue, (1) 459-466 (2000)

(7) K.T. Ooi and G.B. Chai, An analytical model for a vane spring design, *Int'l Journal of Computer Applications in Technology*, 11(1/2), 98-108 (1998)

(8) K.T. Ooi and T.N. Wong, A computer simulation of a rotary compressor for house-hold refrigerators, *Applied Thermal Engineering*, Vol. 17, No. 1, 65 – 78 (1997)

(9) R. Prakash and R. Singh, Mathematical Modelling and Simulation of Refrigerating Compressors, *Proc. 2nd Purdue Compressor Technology Conf.*, Purdue University, 274-285 (1974)

(10) Hiller, C. Carl, et al. Detailed Modelling and Computer Simulation of Reciprocating Refrigeration Compressors, Proc. 3rd Purdue Compressor Technology Conf., Purdue University, 12-17 (1976)

(11) T. Morel and R. Keribar, Comprehensive Model of a Reciprocating Compressor Applicable to Component Design Issues, Proc. of Int'l Compressor Engineering Conf., Purdue University, 375-384 (1988)

(12) Downing, Ralph C. Fluorocarbon refrigerants handbook. Englewood Cliffs, N.J. Prentice Hall, c1988.

(13) M.J. Box, A new method of constraint optimisation and comparison with other methods, The Computer Journal, 8, 33-41 (1965)

Table 1 Comparison between the experimental and predicted results.
(T_{evap} = - 23.3 °C and T_{cond} = 54.4 °C and T_s = 32.2 °C. Compressor operates at 3600 rev/min. Results are normalized relative to measured results.[7])

	R134a	R22
Normalised shaft power, W_{calc}/W_{exp}	0.895 (-10.5%)	0.935 (-6.5%)
Normalised refrigerant flow rate, $\dot{m}_{calc} / \dot{m}_{\exp}$	0.986 (-1.4%)	1.006 (+0.6%)
Normalised cooling capacity, C_{calc}/C_{exp}	0.995 (-0.05%)	1.013 (-1.3%)
Normalised *COP*, COP_{calc}/COP_{exp}	1.11 (+11.1%)	1.083 (+8.3%)

Table 2 Mechanical analysis of the compressor
(Running on R22, Compressor shaft input power: 180 Watt based on motor efficiency of 80.5%, mechanical efficiency is 76.3% and COP:1.72)

Friction analysis results		
Loss due to Vane side Reactions	0.52290 Watt.	6.97%
Loss due to Vane Tip_Roller force	0.51086 Watt.	6.81%
Loss due to Roller & Ecc friction	0.71959 Watt.	9.59%
Loss due to roller & cyl. head faces	2.65651 Watt.	35.41%
Loss due to Eccentric & cyl. head faces	0.18952 Watt.	2.53%
Loss due to Bearing S & shaft	0.73922 Watt.	9.85%
Loss due to Bearing L & shaft	2.16418 Watt.	28.84%
Total Friction Power	7.50280 Watt.	100.00%
Mechanical Efficiency	76.33086	

Table 3 Explicit constraints set in the optimization study.
(a) Limits for design variables

S/N	Lower Limit	Design variables	Upper limit	Unit
1	12	D_{SB} (S_bearing dia.)	16	mm
2	12	D_{LB} (L_bearing dia.)	16	mm
3	25	D_r (roller dia.)	35	mm
4	30	D_c (cylinder dia.)	45	mm
5	D_c-D_r +D_s	D_e (eccentric dia.)	D_r	mm
6	6	D_{sp} (suction port dia.)	12	mm
7	2	D_{dp} (Discharge port dia.)	4	mm
8	1000	K_s (spring stiffness)	9000	N/m
9	0.2	V_t (reed thickness)	0.4	mm
10	3	V_w (reed width)	5	mm
11	15	V_l (reed length)	25	mm
12	4.2	V_r (reed tip radius)	8	mm

Note that h_b is not treated as a free variable but is varied to keep the swept volume constant.

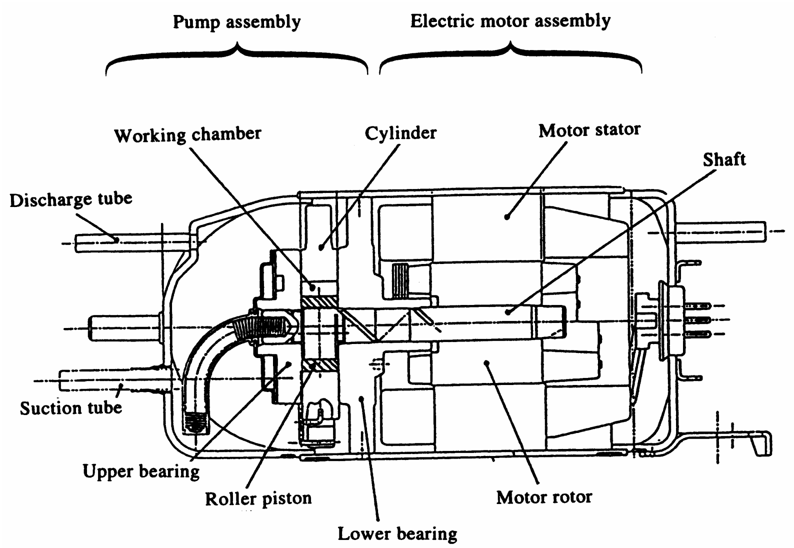

Fig. 1 A rolling piston compressor

Table 4 Geometrical constraints set in the optimization study.

(a) Limits for design variables

S/N	Lower Limit	Design variables	Upper limit	Unit
1	0.1	$= D_e - (D_c - D_r + D_s) =$	*8*	mm
2	1.0	$= (D_c - D_r) =$	**8**	mm
3	1.0	$= (D_c - D_e) =$	**8**	mm
4	1.0	$= (D_c - D_s) =$	**8**	mm
5	0.0	$= (D_r - D_e) =$	8	mm
6	0.0	$= (D_r - D_s) =$	8	mm
7	0.0	$= (D_e - D_s) =$	8	mm
8	35	$= V/(\frac{p}{4}(D_c^2 - D_r^2) =$	55	mm

Note: The swept volume is kept constant by varying the cylinder height.

Table 5 Changes of the dimensions and the performance parameters after optimisation

PARAMETER	**Dia_Bear_S**	**Dia_Bear_L**	**Roller_Dia**	**Cyl_Dia**	**Eccen_Dia**	**SP_Dia**
RATIO(OPT/INIT)	0.858	0.857	0.807	0.825	1.144	1.332
PARAMETER	**Valve_DD**	**SpringK**	**ValveTipRad**	**ValveLength**	**Valve_Width**	**Valve_Thick**
RATIO(OPT/INIT)	1.427	8.041	0.934	1.297	0.717	0.989
PARAMETER	**hb**	**Vane_Side_Frcit**	**Vane_Tip_Frict**	**Roller_Eccen_Fric**	**Roller_Cyl_face**	**Eccen_Cyl_face**
RATIO(OPT/INIT)	1.333	0.055	35.222	0.101	1.787	0.674
PARAMETER	**Shaft_Bear_S**	**Shaft_Bear_L**	**Tot_Frict_Power**	**Volume_Max**	**Overall_Eff**	**COP**
RATIO(OPT/INIT)	0.632	0.630	0.326	1.001	1.120	1.137
PARAMETER	**Refrig_capacity**	**Eff_Mech**	**Work_over_comp**	**Suction_loss**	**hb_Dia_R_ratio**	**Work_ind**
RATIO(OPT/INIT)	1.014	1.105	0.383	0.926	1.616	0.985
PARAMETER	**Vol_eff**	**Rmass_rate**	**hb_**			
RATIO(OPT/INIT)	1.013	1.014	1.333			

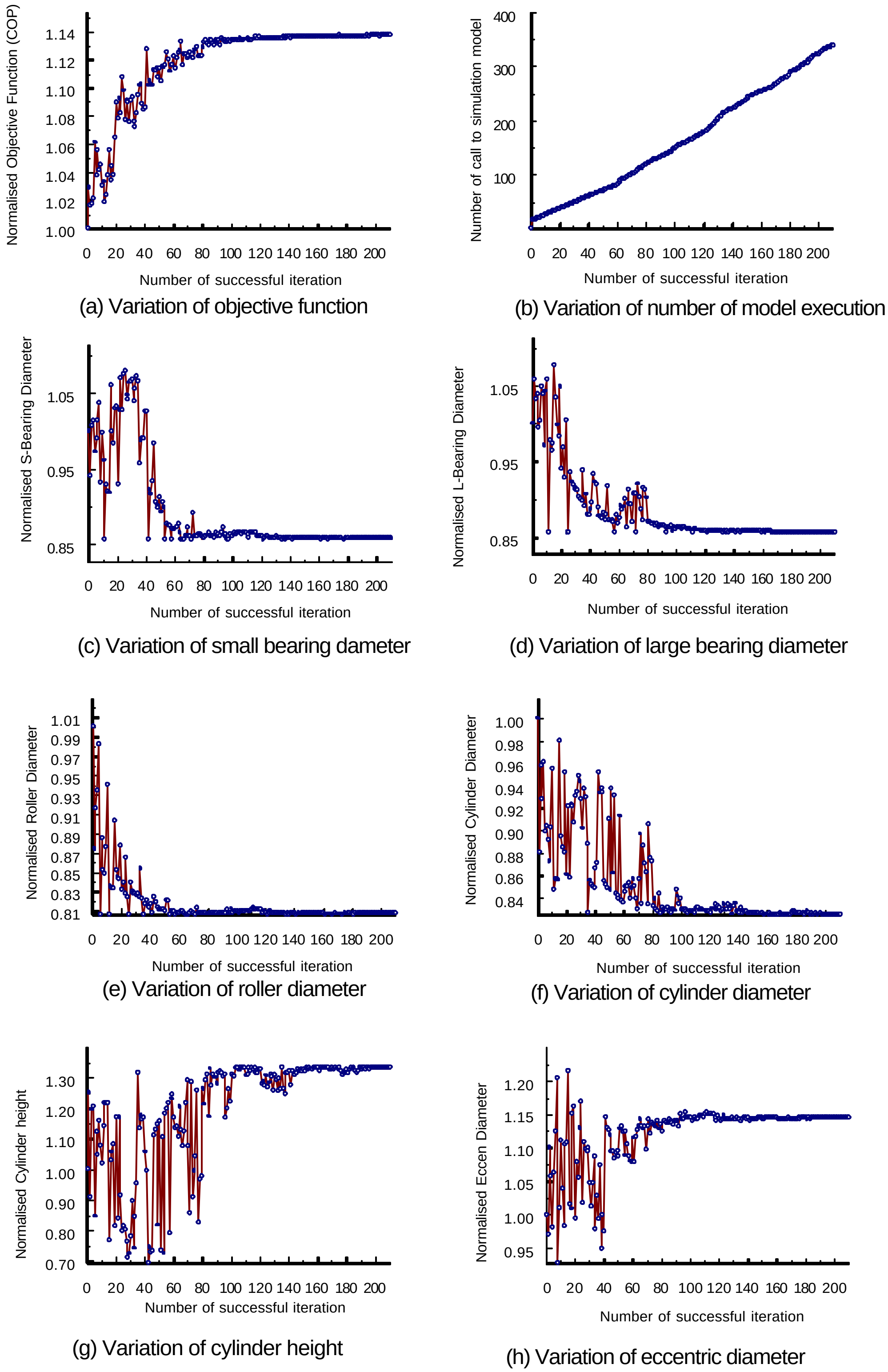

Figure 2 Variations of normalized free variables during optimization search

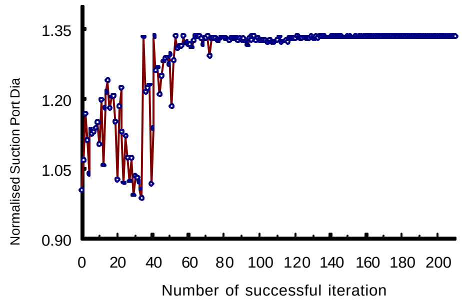

(i) Variation of suction port diameter

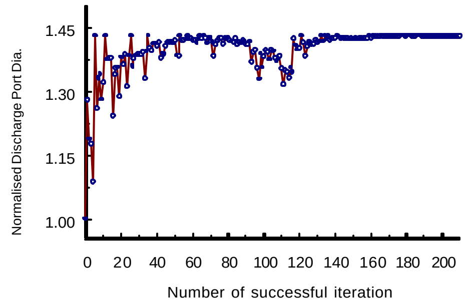

(j) Variation of discharge port diameter

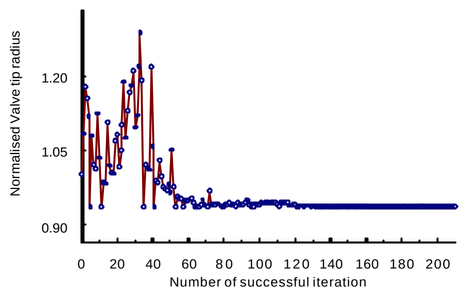

(k) Variation of reed tip radius

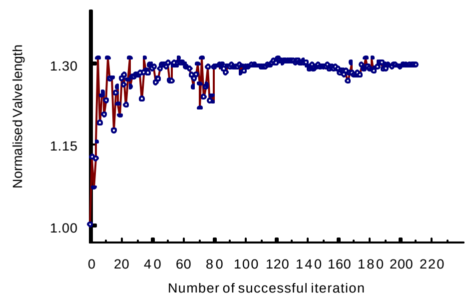

(l) Variation of reed length

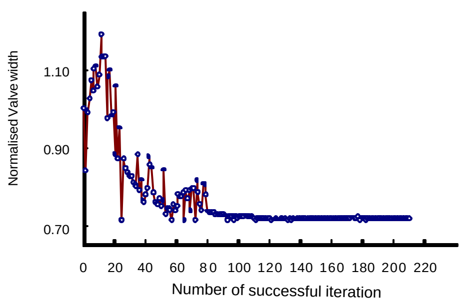

(m) Variation of reed width

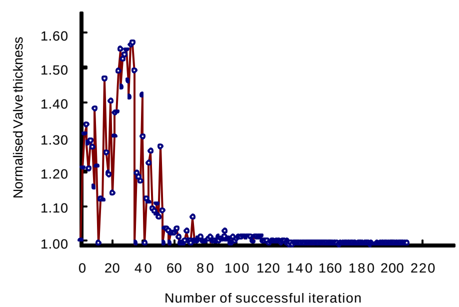

(n) Variation of reed thickness

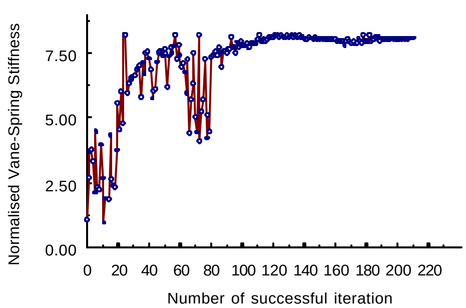

(o) Variation of roller-eccentric clearance

Figure 2 Variations of normalized free variables during optimization search (cont)